Supplementary Information

Multiscale characterization, modeling and simulation of packed bed reactor for direct conversion of syngas to dimethyl ether

Ginu R. George[1], Adam Yonge[2], Meagan F. Crowley[2]*, Anh T. To[3], Peter N. Ciesielski[2]*, Canan Karakaya[1]*

[1]Manufacturing Science Division, Oak Ridge National Laboratory, Oak Ridge, TN, 37830, United States.
[2]Biosciences Center and National Bioenergy Center, National Renewable Energy Laboratory, Golden, CO, 80401, United States.
[3]Catalytic Carbon Transformation & Scale-up Center, National Renewable Energy Laboratory, Golden, CO, 80401, United States.
*Corresponding authors: peter.ciesielski@nrel.gov; karakayac@ornl.gov

S1. Al_2O_3 packed bed MicroCT characterization

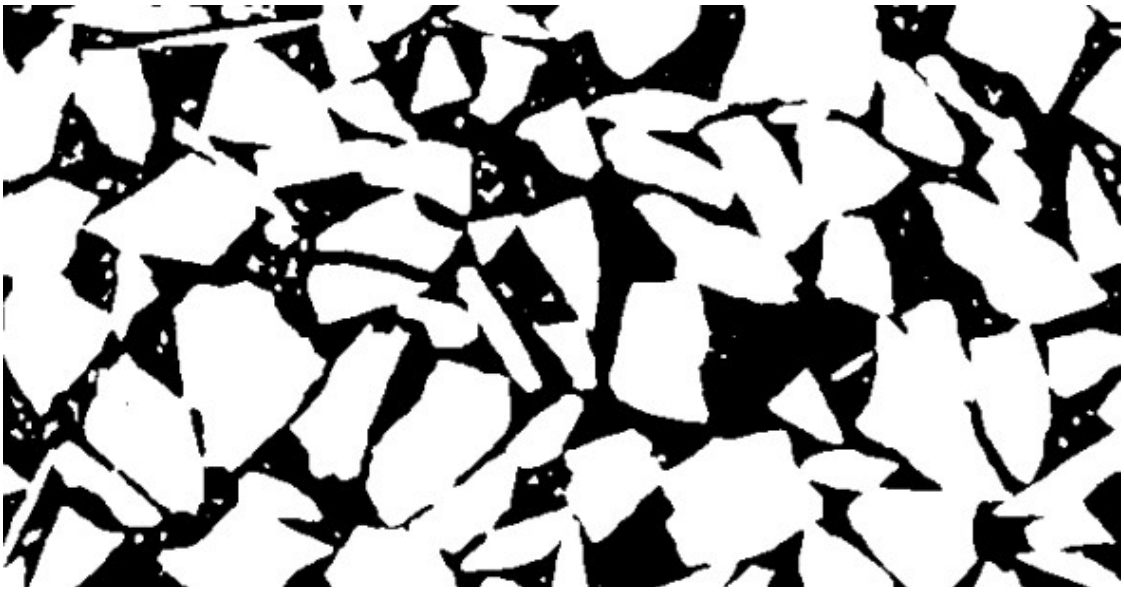

Figure S1: Example visual slice of the Al2O3 packed bed processed using MicroCT and MATBOX postprocessing.

Table S1: List of physical properties of the Al_2O_3 packed bed found using the MATBOX software. Here directions 1, 2, 3 denote various directions along the geometric space, with 1 representing the length of the bed.

Direction	Volume Fraction	Tortuosity	Bruggeman exponent	Normalized D_{eff}
1	0.371	2.01	1.71	0.185
2	0.371	1.87	1.62	0.199
3	0.371	2.02	1.70	0.184

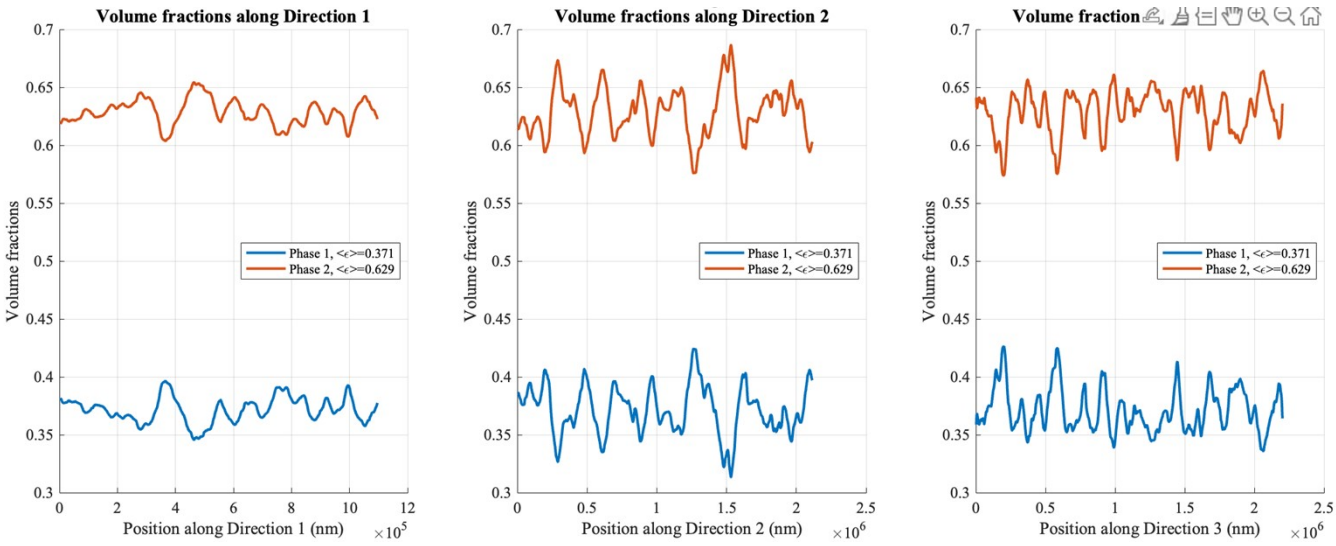

Figure S2: Volume fraction of the packed bed consisting of Al_2O_3 particles. An average bed porosity of 0.371 was observed in this configuration. Phases 1 and 2 represent the open and solid spaces, respectively.

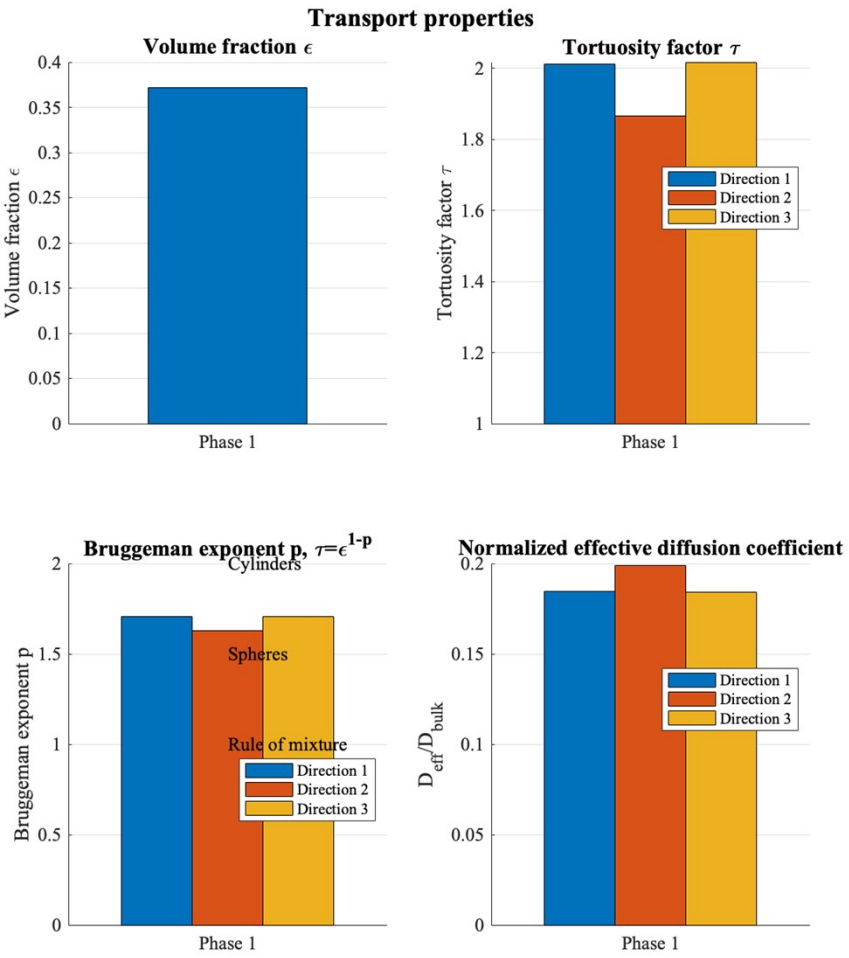

Figure S3: Tortuosity and effective diffusivity coefficient of the packed bed consisting of Al_2O_3 particles along three directions.

Table S2: Particle size distribution (phase 2) of the Al_2O_3 packed bed calculated using the CPSD algorithm. The standard deviations (Std) of the calculated values are represented as lengths and percentages. Phase 1 represents the open space (void).

Phase	Min (nm)	Mean (nm)	Max (nm)	Std (nm)	Std (%)
1	6.35E3	4.81E4	1.13E5	1.72E4	35.7
2	6.35E3	1.14E5	2.66E5	4.48E4	39.2

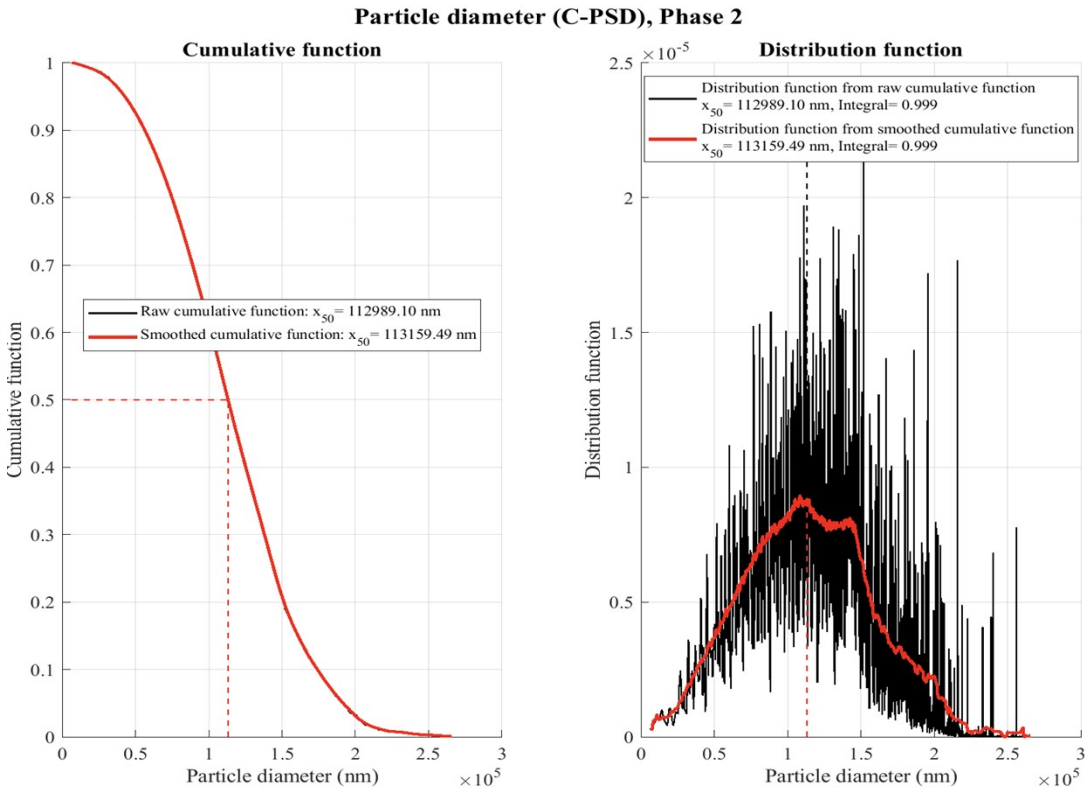

Figure S4: Visual of the $Al2O_3$ particle size distribution in the packed bed calculated using the CPSD algorithm.

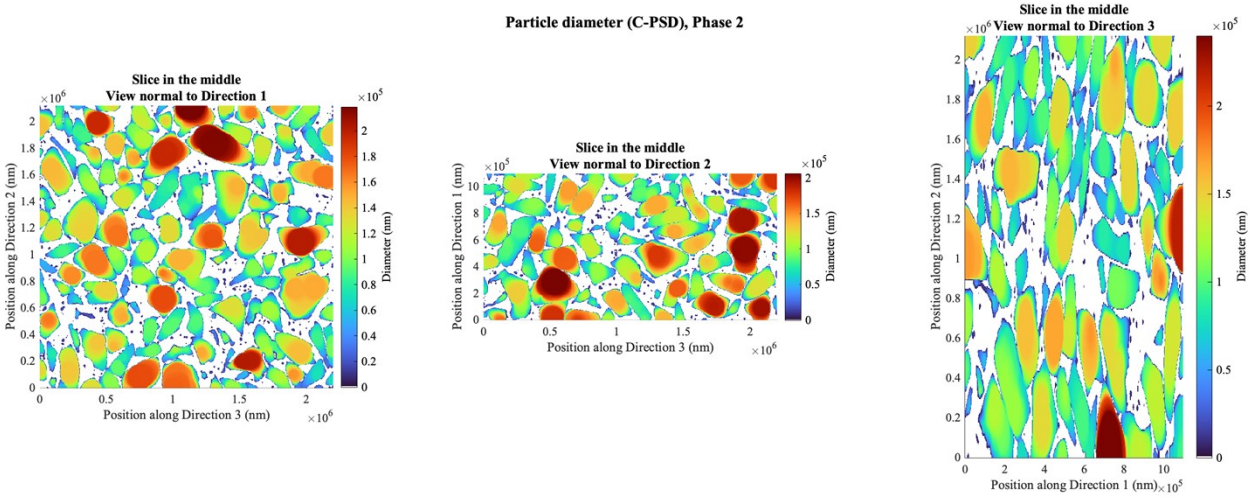

Figure S5: Heat map of the Al_2O_3 particle size distribution using the CPSD algorithm.

Table S3: Particle size distribution (phase 2) of the Al_2O_3 packed bed calculated using the EDMF algorithm. The standard deviations (Std) of the calculated values are represented as lengths and percentages. Phase 1 represents the open space (void).

Phase	Min (nm)	Mean (nm)	Max (nm)	Std (nm)	Std (%)
1	3.17E3	1.08E4	5.66E5	6.50E4	60.4
2	3.17E3	2.15E5	1.32E5	1.59E4	74.0

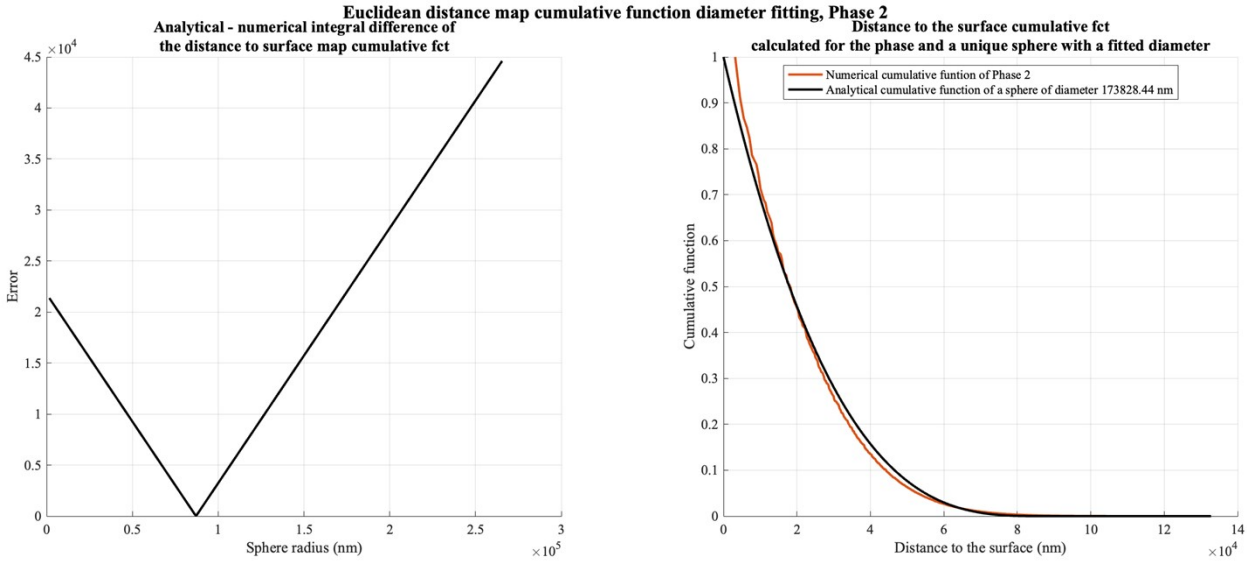

Figure S6: Visual of the $Al2O_3$ particle size distribution in the packed bed calculated using the EDMF algorithm.

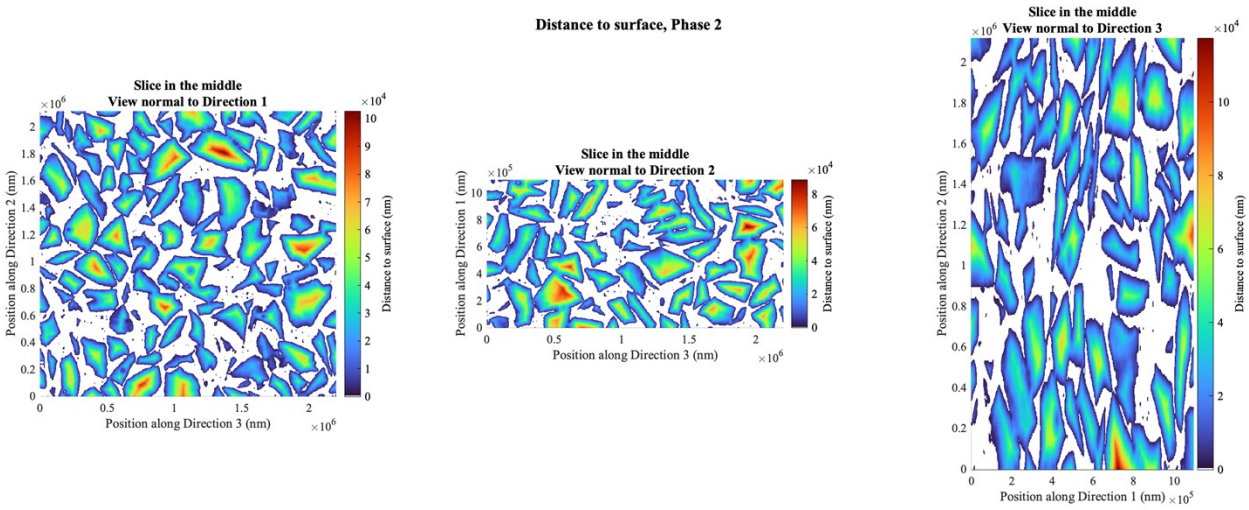

Figure S7: Heat map of the Al_2O_3 distance to surface distribution using the EDMF algorithm.

S2. CZA packed bed MicroCT characterization

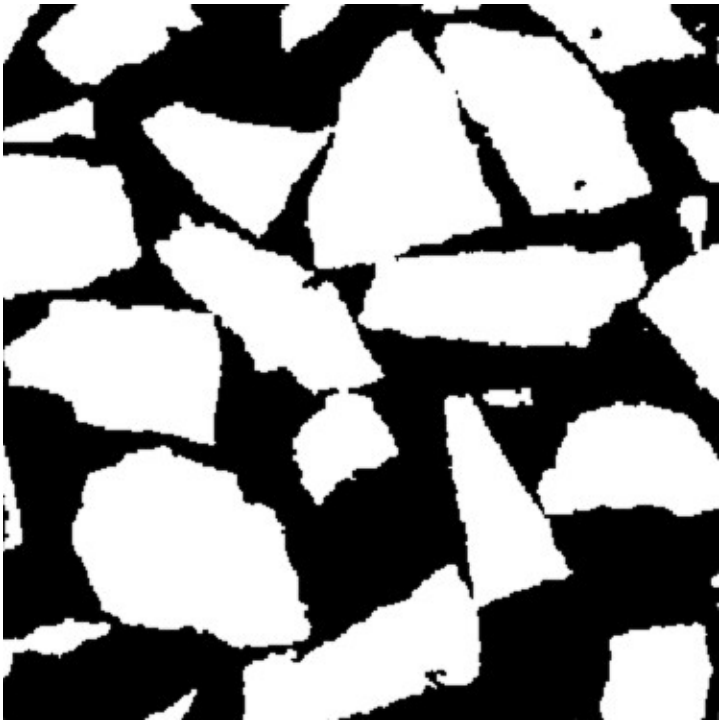

Figure S8: Example visual slice of the CZA packed bed reactor processed using MicroCT and MATBOX postprocessing.

Table S4: List of physical properties of the CZA packed bed found using the MATBOX software. Here directions 1, 2, 3 denote various directions along the geometric space, with 1 representing the length of the bed.

Direction	Volume Fraction	Tortuosity	Bruggeman exponent	Normalized D_{eff}
1	0.446	1.91	1.80	0.233
2	0.446	1.59	1.58	0.278
3	0.446	1.60	1.58	0.278

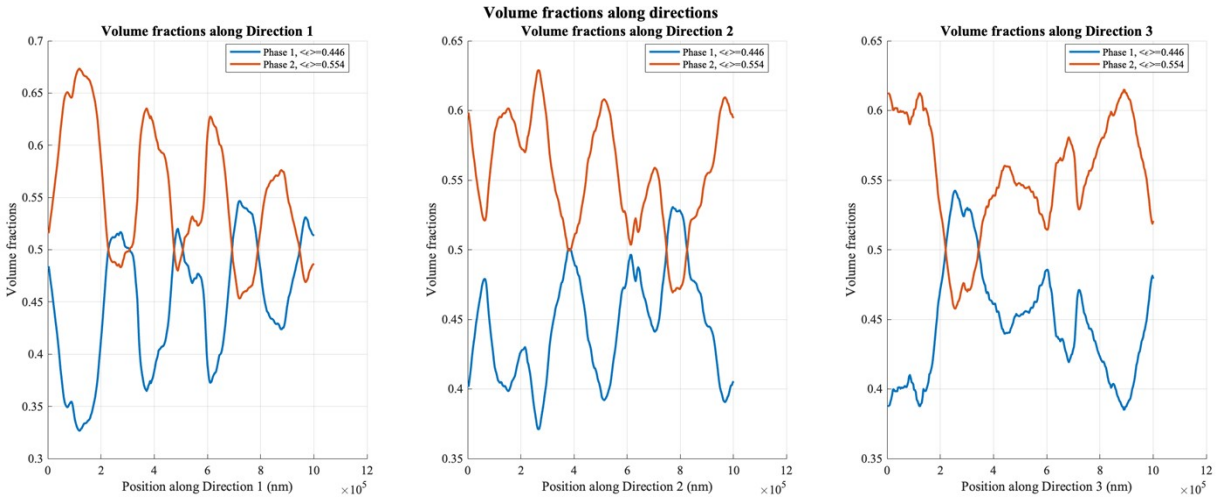

Figure S9: Volume fraction of the packed bed consisting of CZA particles. A porosity of 0.446 was observed in this configuration.

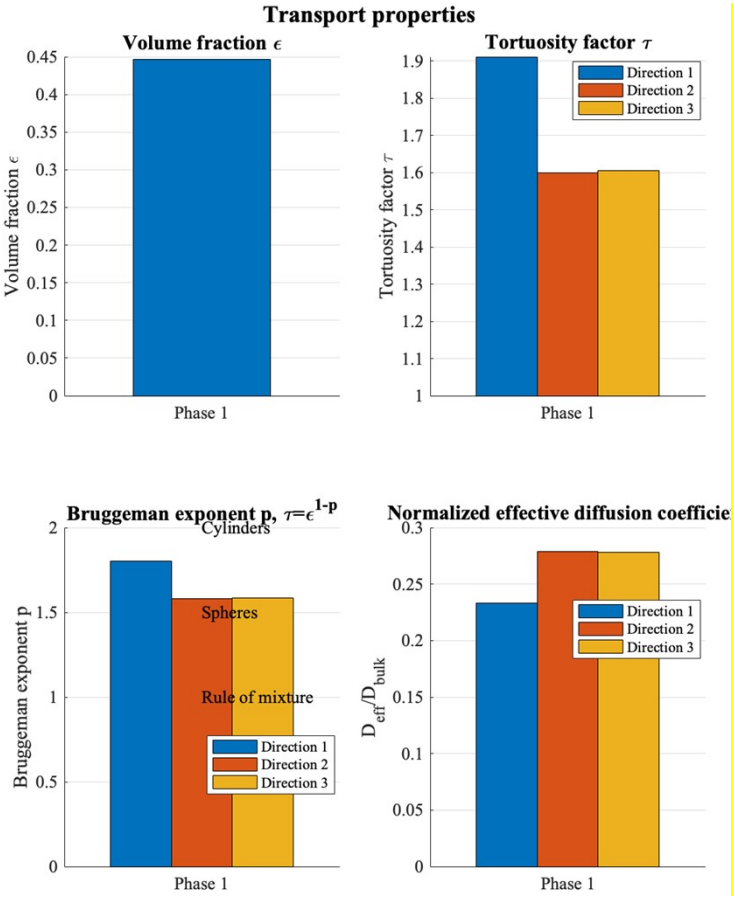

Figure S10: Tortuosity and effective diffusivity coefficient of the packed bed consisting of CZA particles along three directions.

Table S5: Particle size distribution (phase 2) of the CZA in the packed bed reactor calculated using the CPSD algorithm. The standard deviations (Std) of the calculated values are represented as lengths and percentages. Phase 1 represents the open space (void).

Phase	Min (nm)	Mean (nm)	Max (nm)	Std (nm)	Std (%)
1	6.35E3	8.98E4	2.08E5	4.26E4	47.4
2	6.35E3	1.15E5	2.57E5	4.18E4	36.2

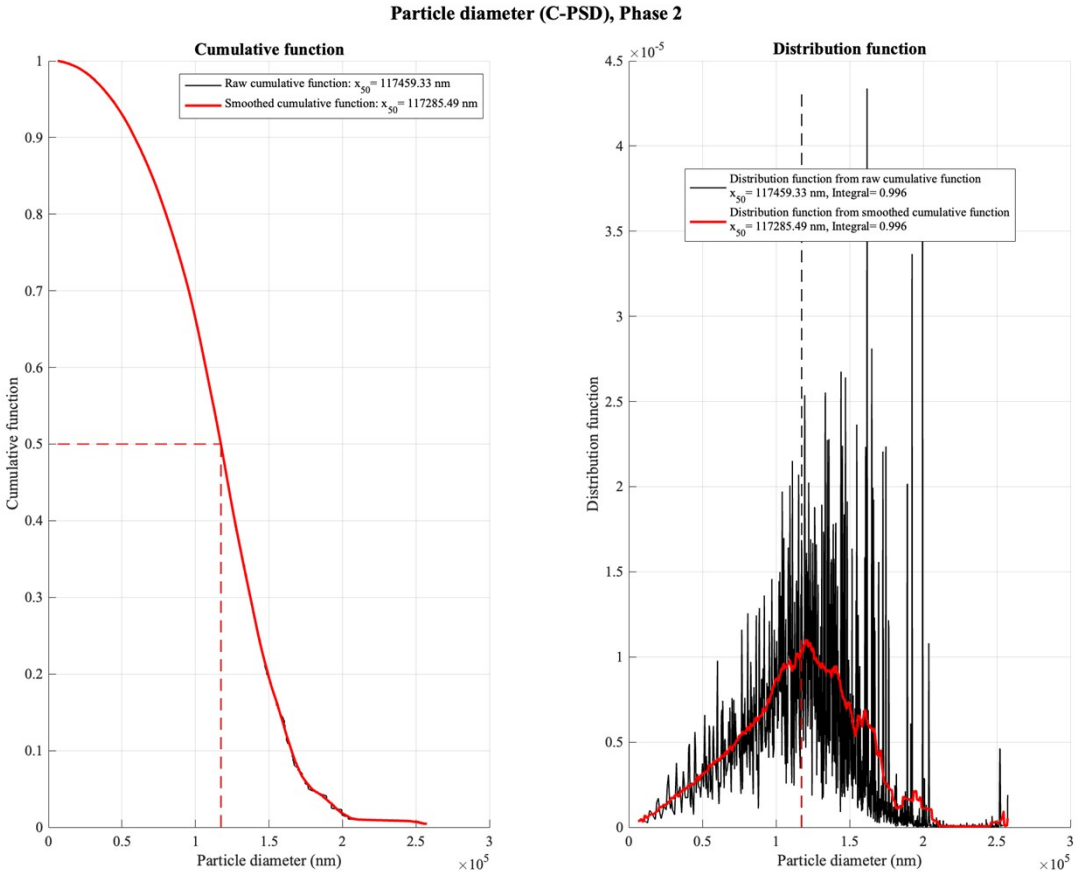

Figure S11: Visual of the CZA particle size distribution in the packed bed calculated using the CPSD algorithm.

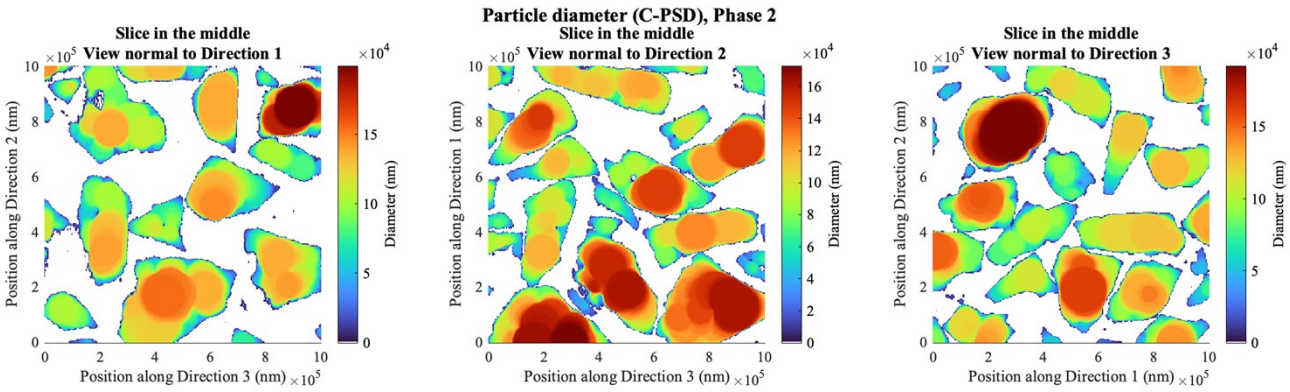

Figure S12: Heat map of the CZA particle size distribution using the CPSD algorithm.

Table S6: Distance to surface distribution (phase 2) of the CZA in the packed bed reactor calculated using the EDMF algorithm. The standard deviations (Std) of the calculated values are represented as lengths and percentages. Phase 1 represents the open space (void).

Phase	Min (nm)	Mean (nm)	Max (nm)	Std (nm)	Std(%)
1	3.18E3	1.84E4	1.04E5	1.36E4	73.7
2	3.18E3	2.26E5	1.28E5	1.60E4	71.0

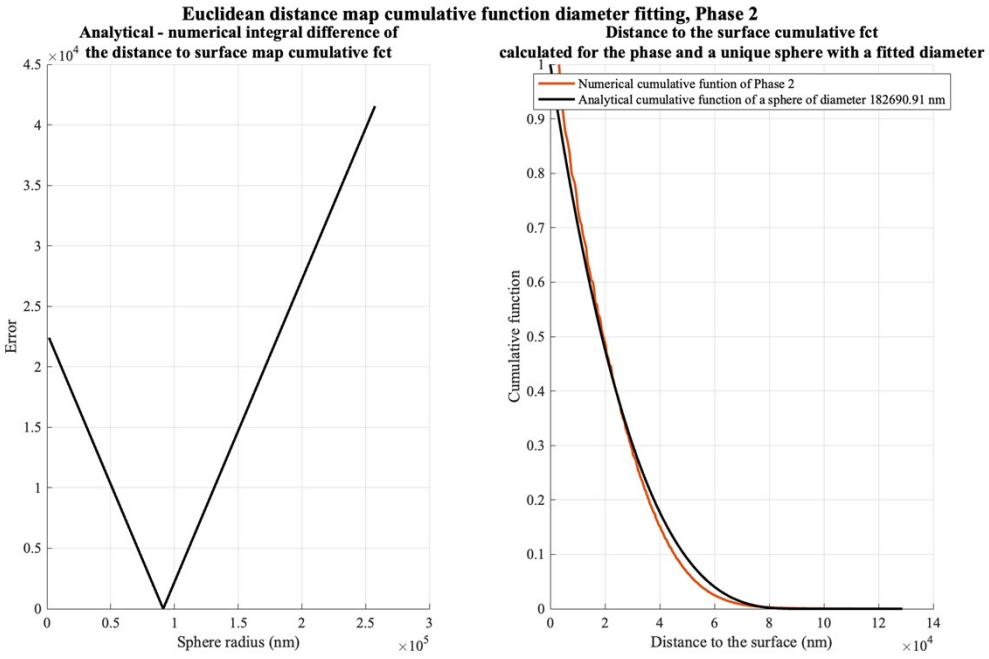

Figure S13: Visual of the CZA particle size distribution in the packed bed calculated using the EDMF algorithm.

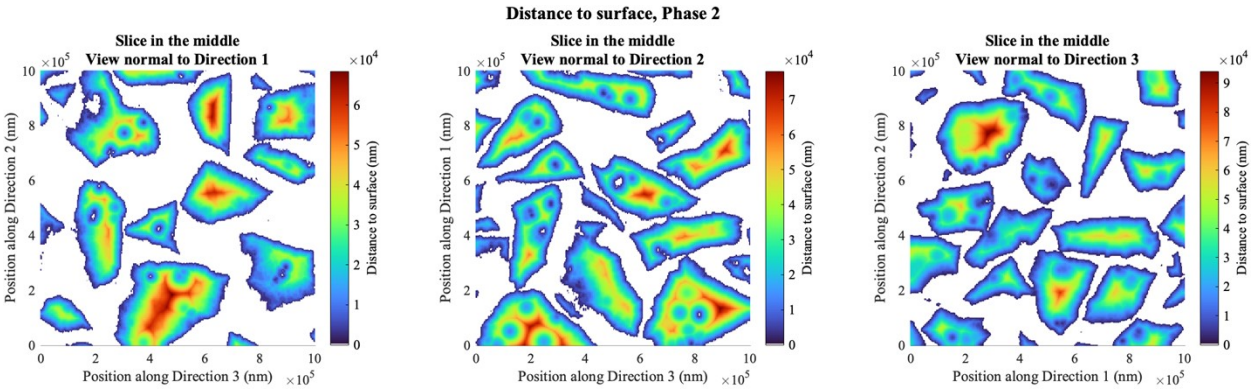

Figure S14: Heat map of the CZA distance to surface distribution using the EDMF algorithm.

S3. CZA and Al_2O_3 mixed packed bed MicroCT characterization

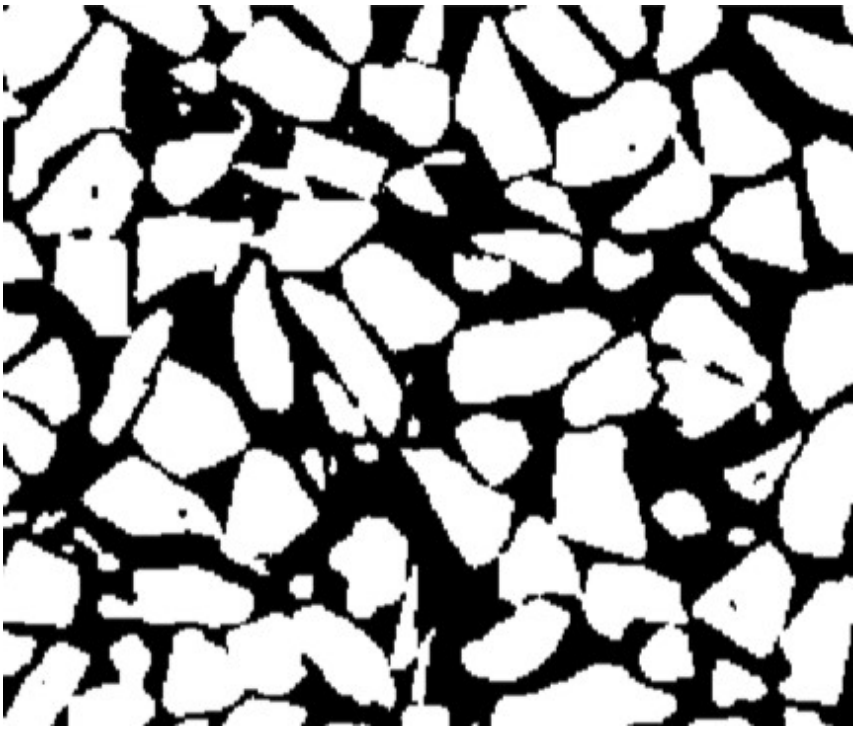

Figure S15: Example visual slice of the mixed packed bed reactor processed using MicroCT and MATBOX postprocessing.

Table S7: List of physical properties of the mixed packed bed found using the MATBOX software. Here directions 1, 2, 3 denote various directions along the geometric space, with 3 representing the length of the bed.

Direction	Volume Fraction	Tortuosity	Bruggeman exponent	Normalized D_{eff}
1	0.397	1.75	1.60	0.227
2	0.397	1.74	1.60	0.228
3	0.397	2.02	1.76	0.197

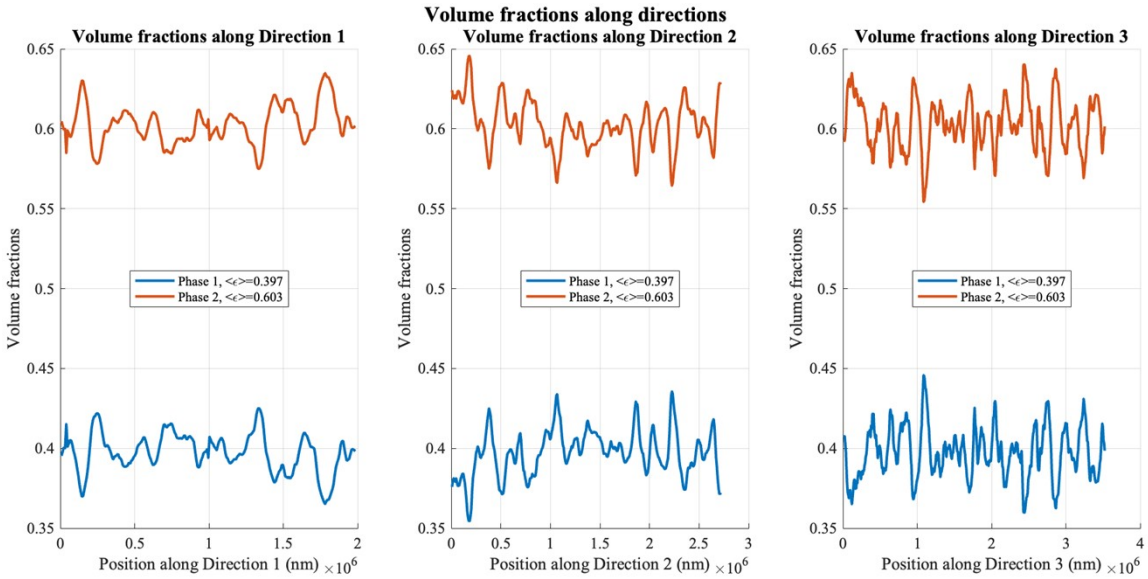

Figure S16: Volume fraction of the packed bed consisting of mixed particles. A porosity of 0.397 was observed in this configuration.

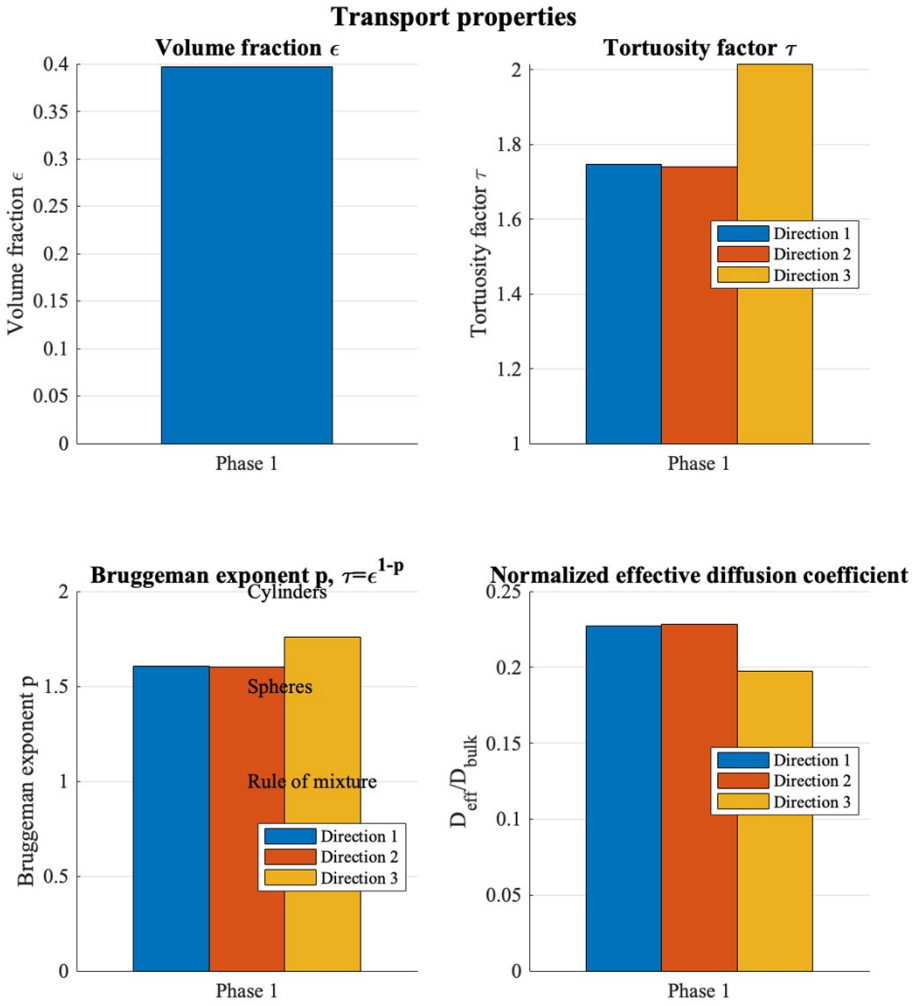

Figure S17: Tortuosity and effective diffusivity coefficient of the packed bed consisting of mixed particles along three directions.

S4. Al_2O_3 pellet NanoCT characterization

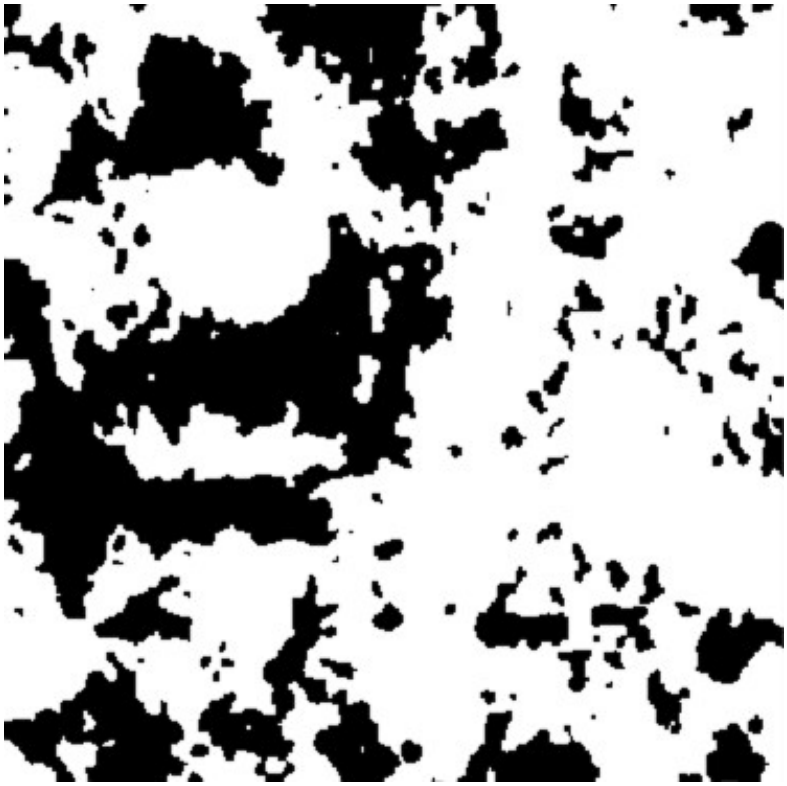

Figure S18: Example visual slice of the Al_2O_3 pellet processed using NanoCT and MATBOX postprocessing.

Table S8: List of physical properties of the Al_2O_3 pellet found using the MATBOX software.

Direction	Volume Fraction	Tortuosity	Bruggeman exponent	Normalized D_{eff}
1	0.384	3.36	2.26	0.114
2	0.384	10.49	3.45	0.037
3	0.384	3.79	2.39	0.101

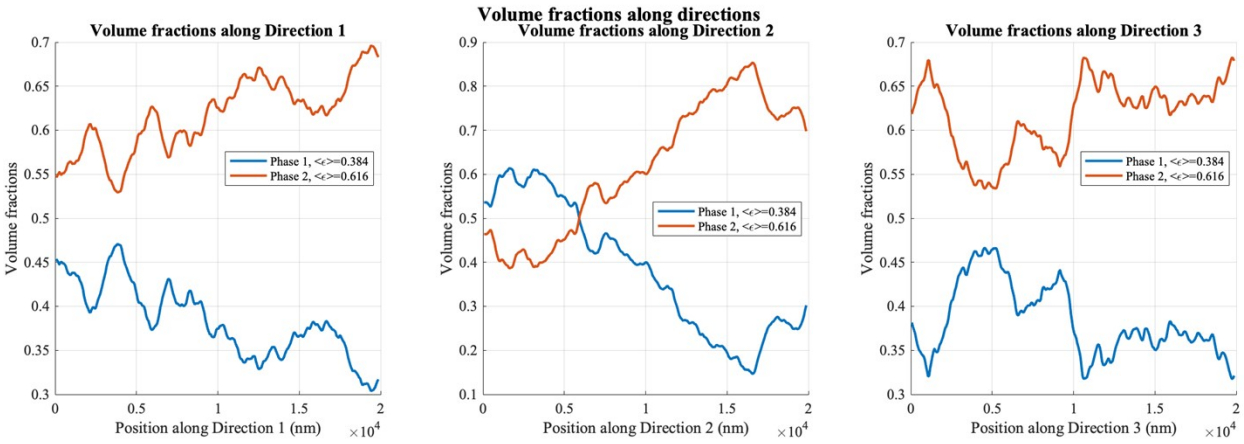

Figure S19: Volume fraction of the Al_2O_3 pellet. A porosity of was 0.384 observed in this configuration.

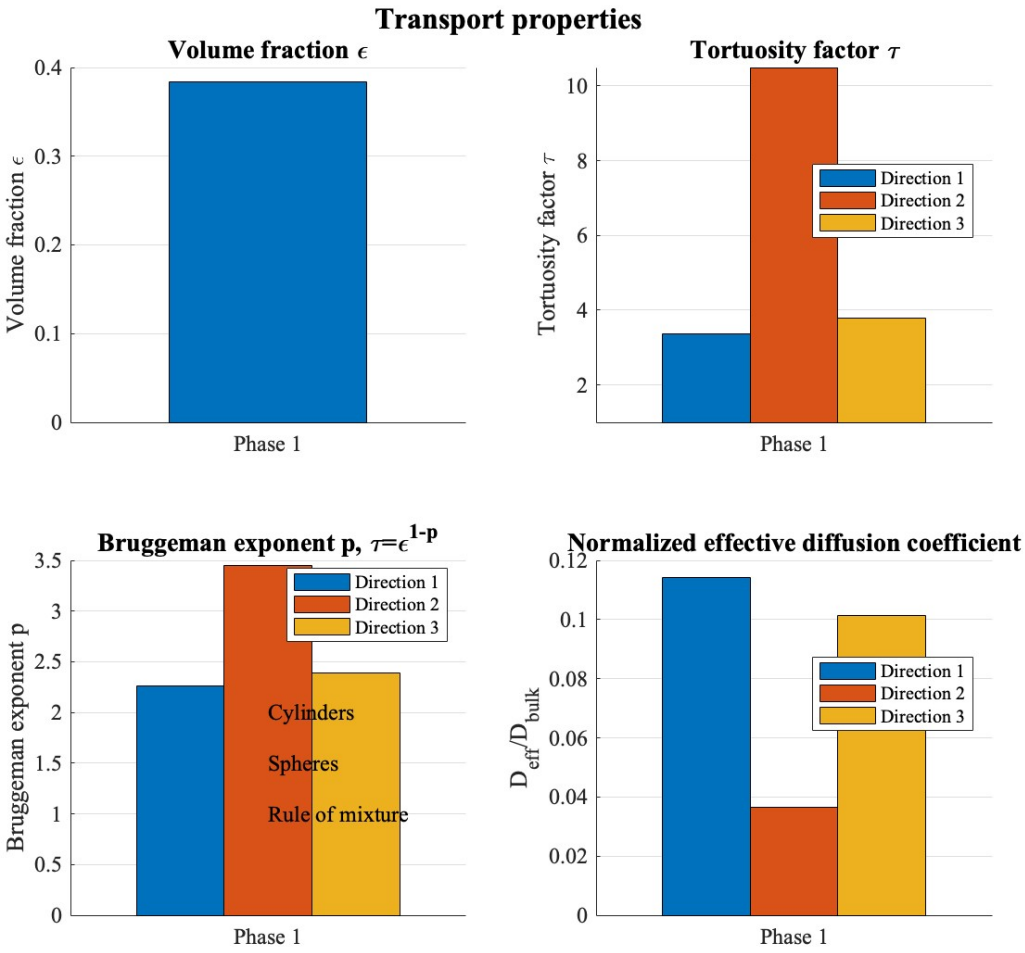

Figure S20: Tortuosity and effective diffusivity coefficient of the Al_2O_3 pellet along three directions.

Table S9: Pore distribution (phase 1) of the Al_2O_3 pellet calculated using the CPSD algorithm.

Phase	Min (nm)	Mean (nm)	Max (nm)	Std (nm)	Std(%)
1	1.32E2	1.20E3	3.92E3	8.85E2	73.6
2	1.32E2	1.23E3	4.13E3	6.52E2	53

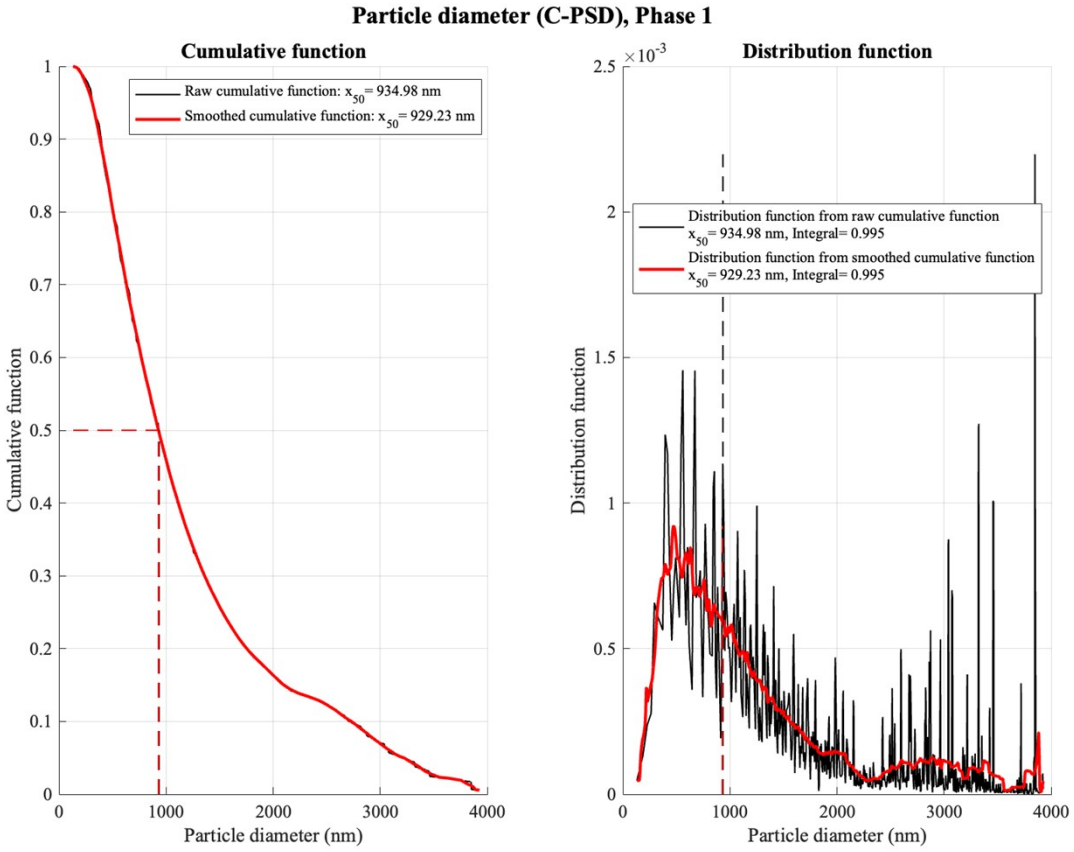

Figure S21: Visual of the Al_2O_3 pellet pore size distribution using the CPSD algorithm.

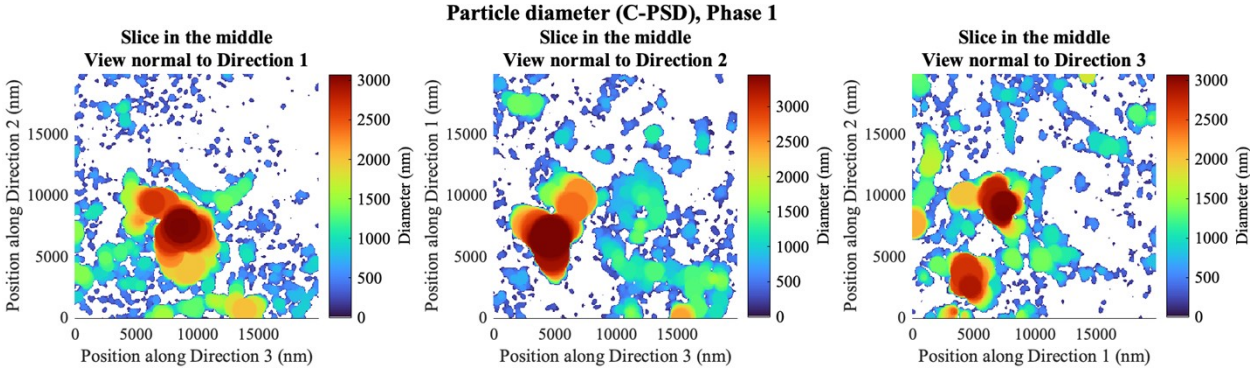

Figure S22: Heat map of the Al_2O_3 pellet pore size distribution using the CPSD algorithm.

Table S10: Pore size distribution (phase 1) of the Al_2O_3 pellet calculated using the EDMF algorithm.

Phase	Min nm	Mean nm	Max nm	Std nm	Std%
1	6.60E1	2.55E2	1.96E3	2.33E2	91.4
2	6.60E1	2.71E2	2.06E3	1.94E2	71.6

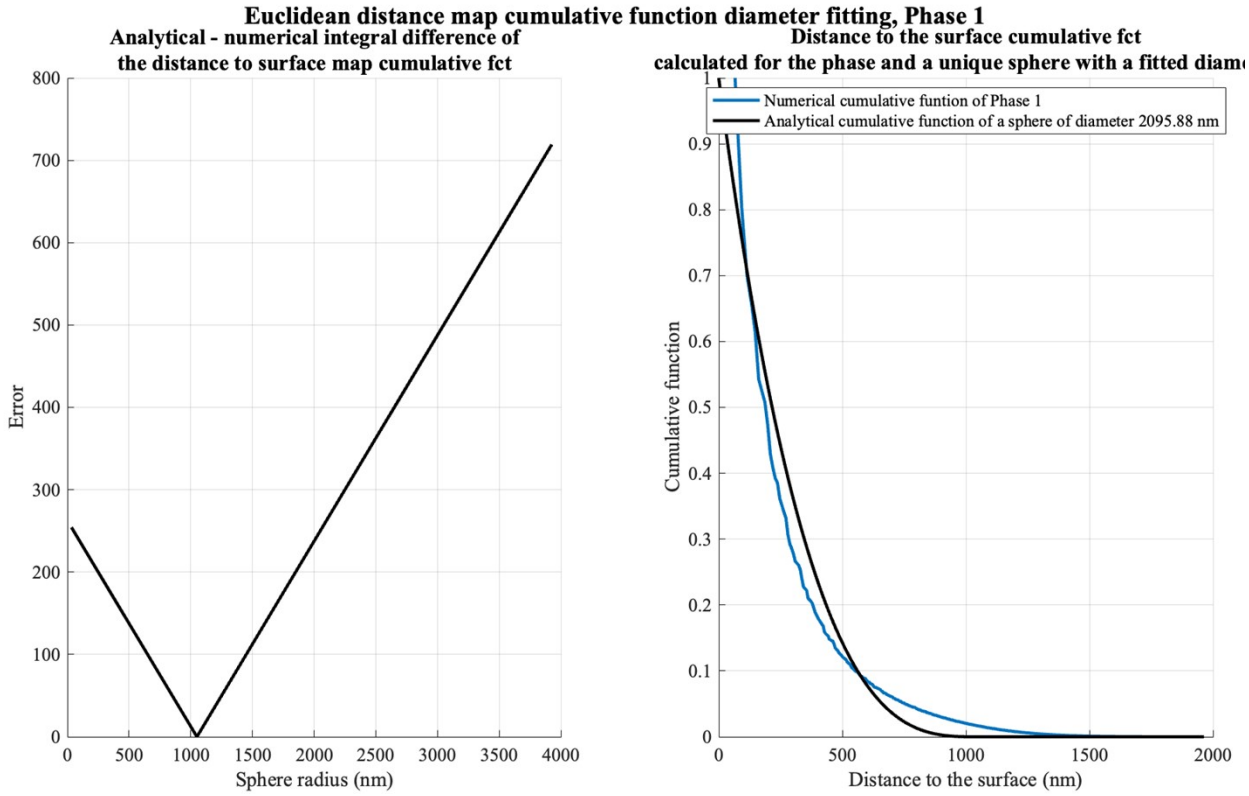

Figure S23: Visual of the Al_2O_3 particle size distribution in the packed bed calculated using the EDMF algorithm.

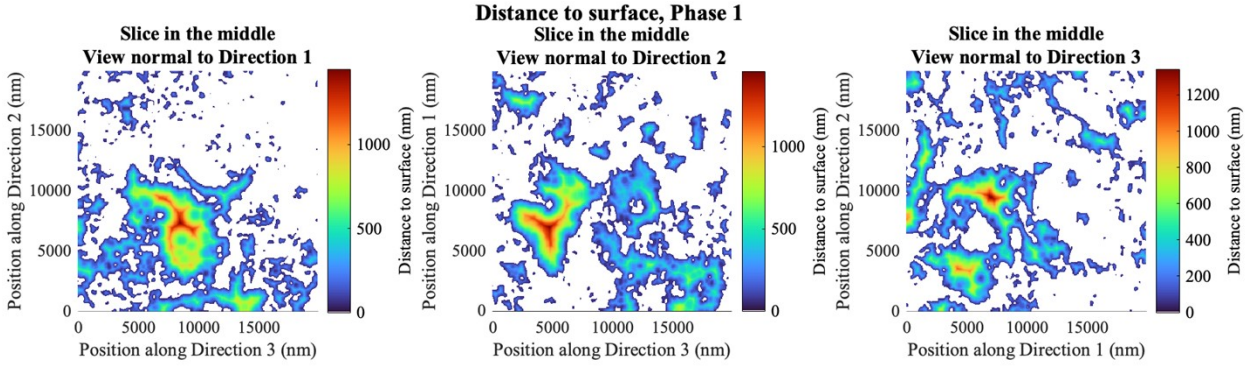

Figure S24: Heat map of the Al_2O_3 distance to surface distribution using the EDMF algorithm

S5. CZA pellet NanoCT characterization

Figure S25: Example visual slice of the CZA pellet processed using NanoCT and MATBOX postprocessing.

Table S11: List of physical properties of the CZA pellet found using the MATBOX software.

Direction	Volume Fraction	Tortuosity	Bruggeman exponent	Normalized D_{eff}
1	0.293	3.70	2.06	0.079
2	0.293	4.28	2.19	0.069
3	0.293	3.08	1.92	0.095

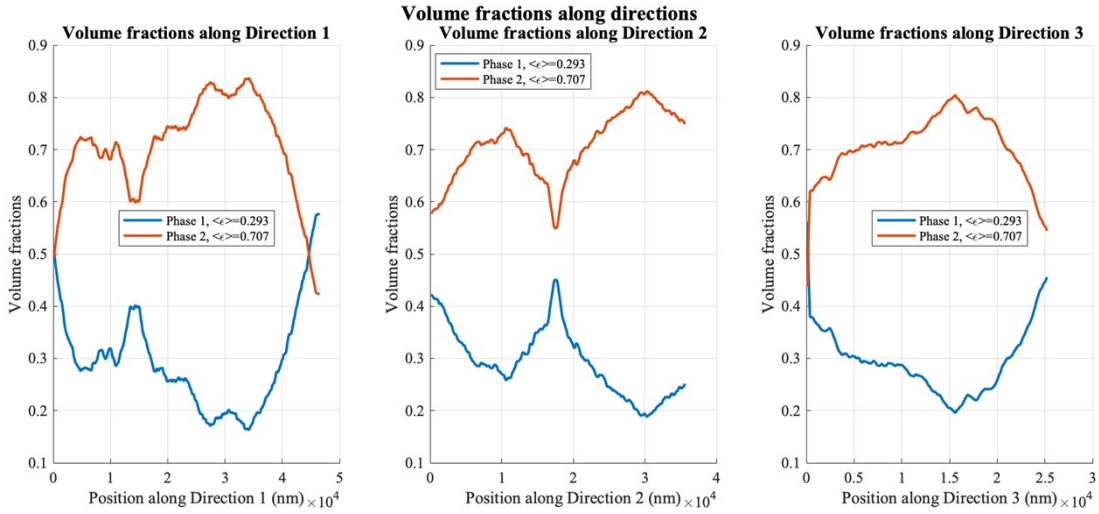

Figure S26: Volume fraction of the CZA pellet. A porosity of 0.293 was observed in this configuration.

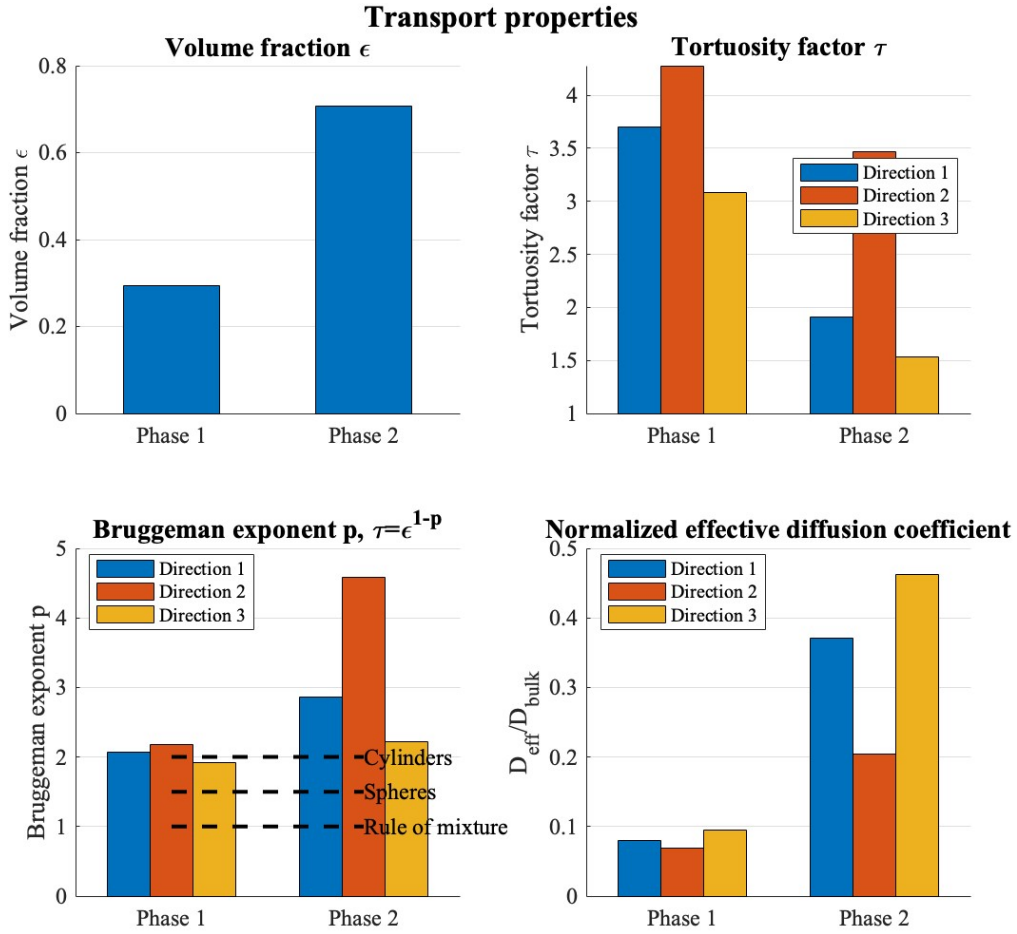

Figure S27: Tortuosity and effective diffusivity coefficient of the CZA pellet along three directions.

Table S12: Pore distribution (phase 1) of the CZA pellet calculated using the CPSD algorithm. Phase 2 represents the solid phase.

Phase	Min nm	Mean nm	Max nm	Std nm	Std%
1	2.56E2	1.48E3	1.25E4	1.72E3	115.9
2	2.56E2	2.28E3	9.22E3	1.87E3	82.0

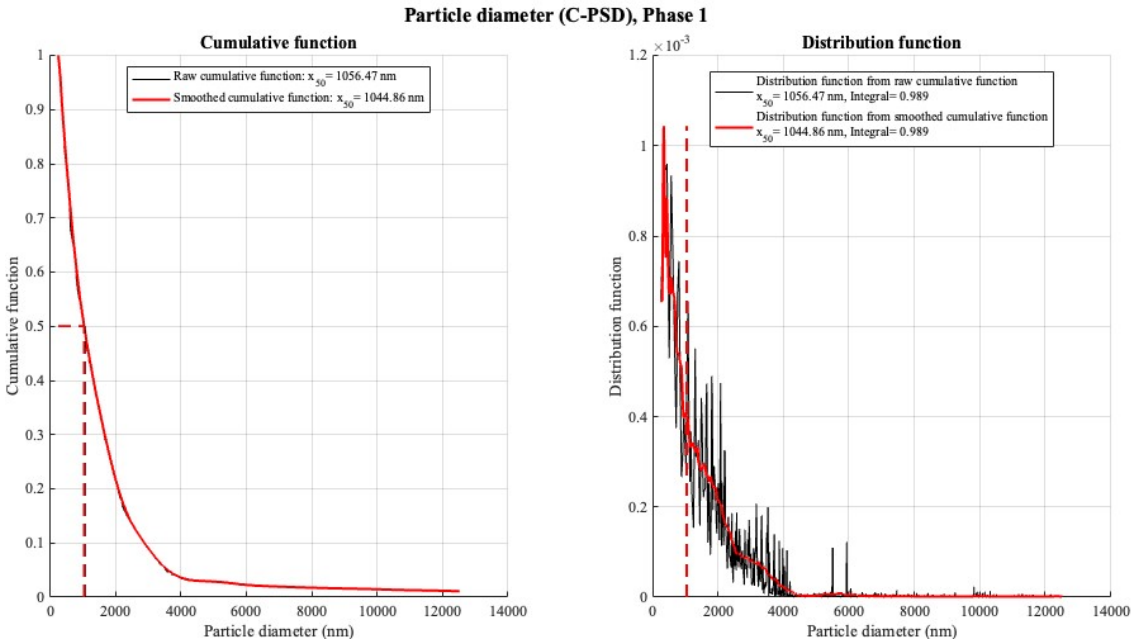

Figure S28: Visual of the CZA pellet pore size distribution using the CPSD algorithm.

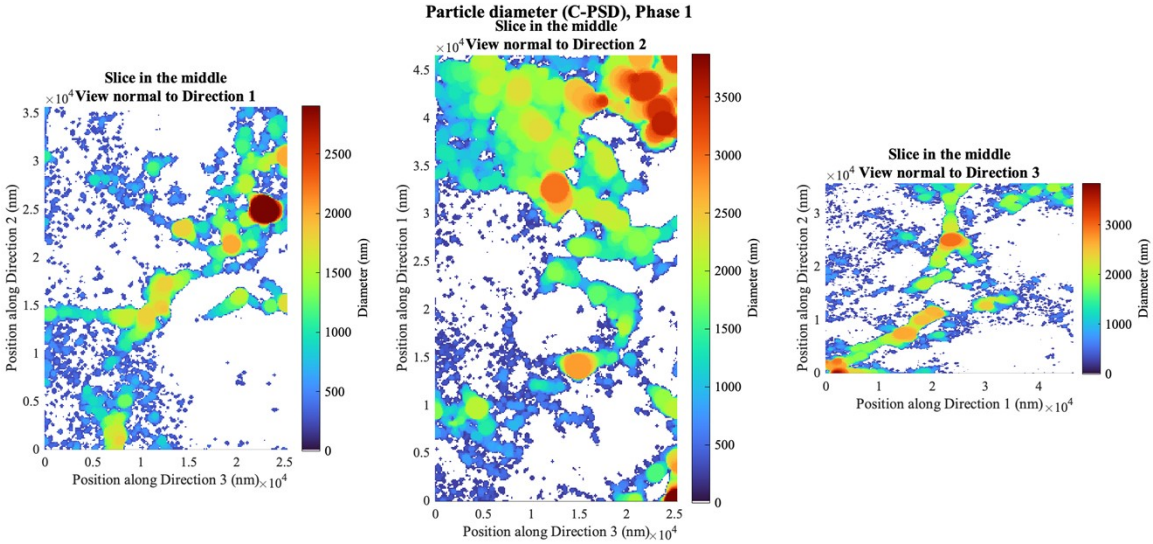

Figure S29: Heat map of the CZA pellet pore size distribution using the CPSD algorithm.

Table S13: Pore size distribution (phase 1) of the CZA pellet calculated using the EDMF algorithm.

Phase	Min nm	Mean nm	Max nm	Std nm	Std%
1	1.28E2	3.39E2	6.26E3	3.17E2	109.7
2	1.28E2	5.14E2	4.61E3	4.79E2	93.2

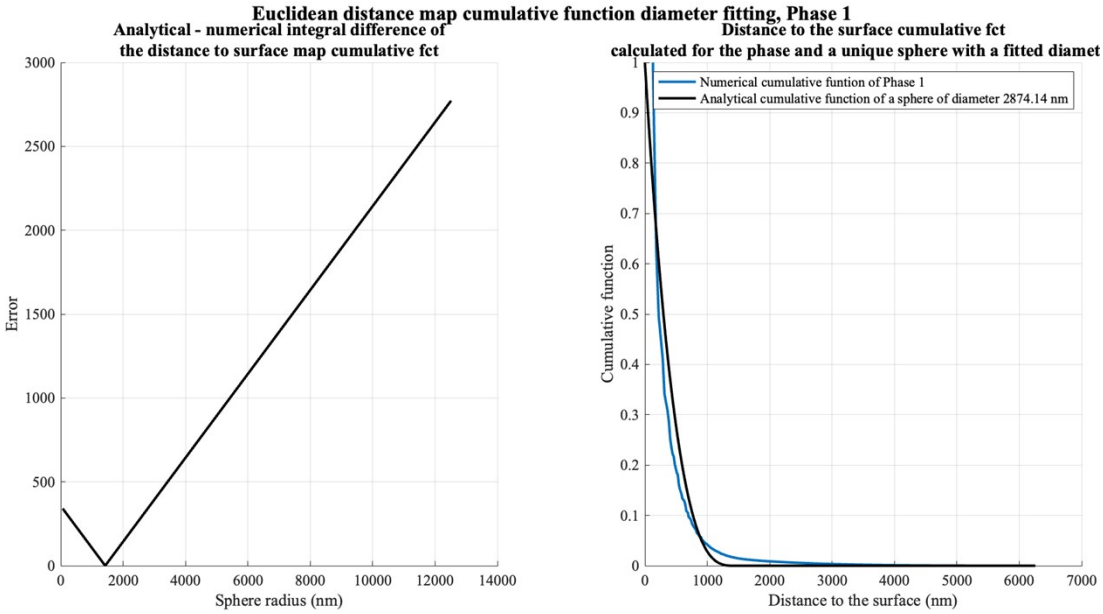

Figure S30: Visual of the CZA particle size distribution in the packed bed calculated using the EDMF algorithm.

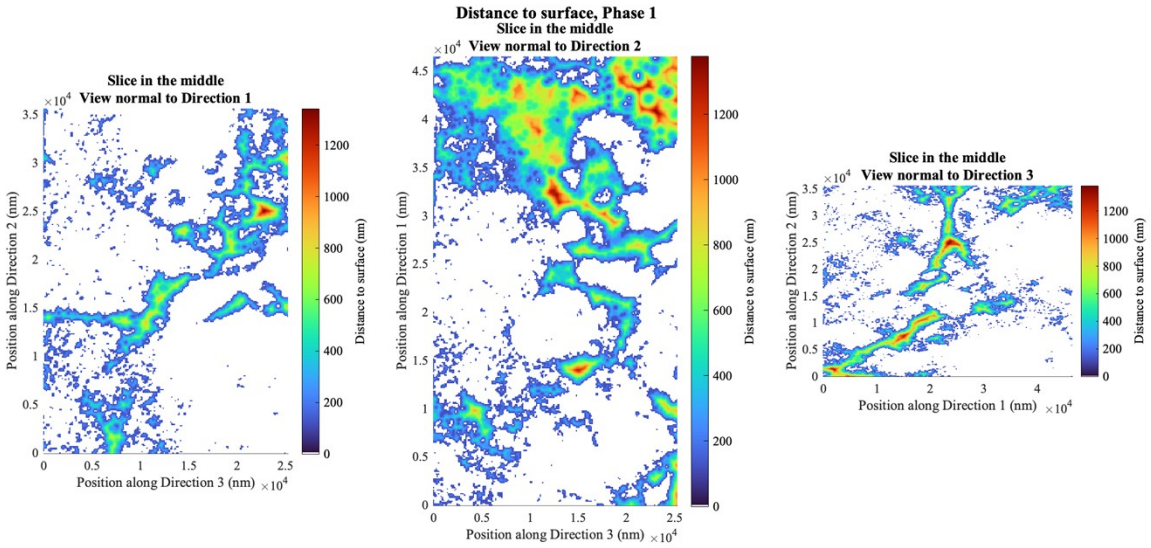

Figure S31: Heat map of the CZA distance to surface distribution using the EDMF algorithm

S6. Al_2O_3 TEM characterization

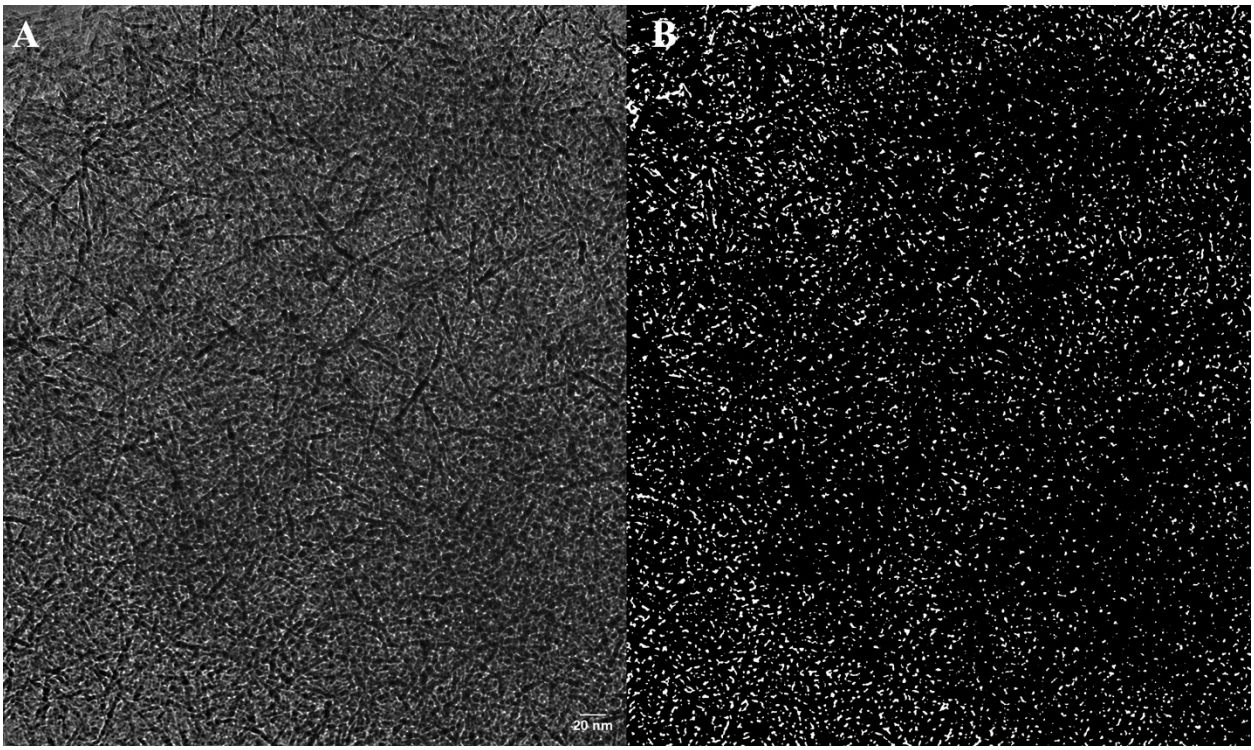

Figure S32: A TEM scan (A) and the associated binary reconstruction (B) of the Al_2O_3 at 25x magnification

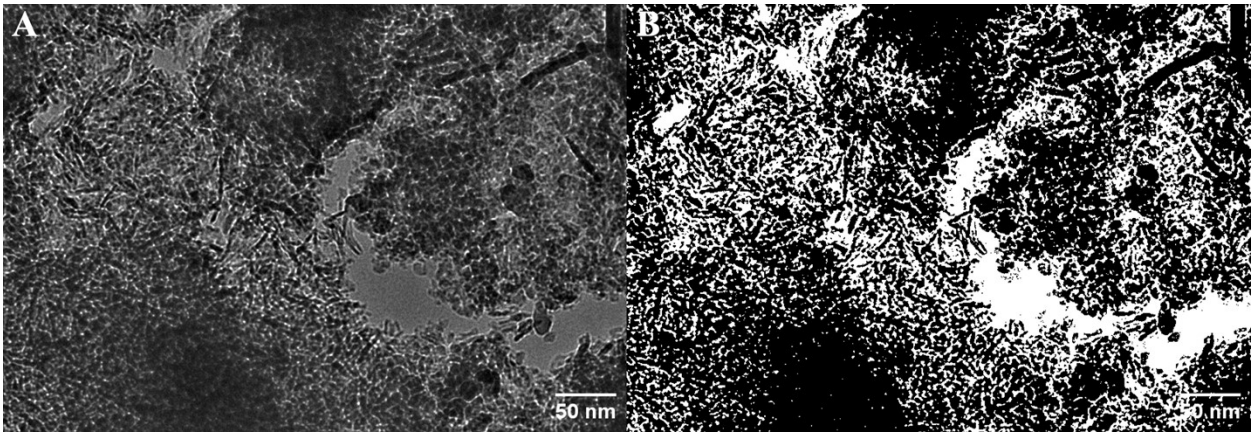

Figure S33: A TEM scan (A) and the associated binary reconstruction (B) of the Al_2O_3 at 11.5x magnification

Table S14: Al_2O_3 pore size and porosity analysis of TEM images. Images 13xx (11.5x magnification) and 14xx (25x magnification) cover different areas (2 to 3 times difference) and their individual averages were calculated.

Image	Count	Total Area (nm^2)	Average Size (nm)	% Area
1370	4769	55824	11.706	31.36
1371	4561	54284	11.902	26.61
1372	2236	37886	16.94	29.98
1373	6370	71669	11.25	33.817
1374	6301	48015	7.62	18.488
1375	5185	42323	8.163	13.5
1376	5792	67377	11.63	22.385
1377	8304	80008	9.635	27.411
1393	7348	80469	10.95	20.94
1394	5394	64083	11.88	20.137
1407	7649	18980	2.481	7.043
1408	4418	5405	1.224	2.006
1409	7700	21291	2.765	7.9
1422	3345	12180	3.641	4.519
1423	3735	15064	4.033	5.919
Average	**5540**	**44990**	**8.388**	**18.134**
13xx Average (lower mag)	5626	60194	11.168	24.463
14xx Average (higher mag)	5369.4	14584	2.829	5.477

S7. CZA TEM characterization

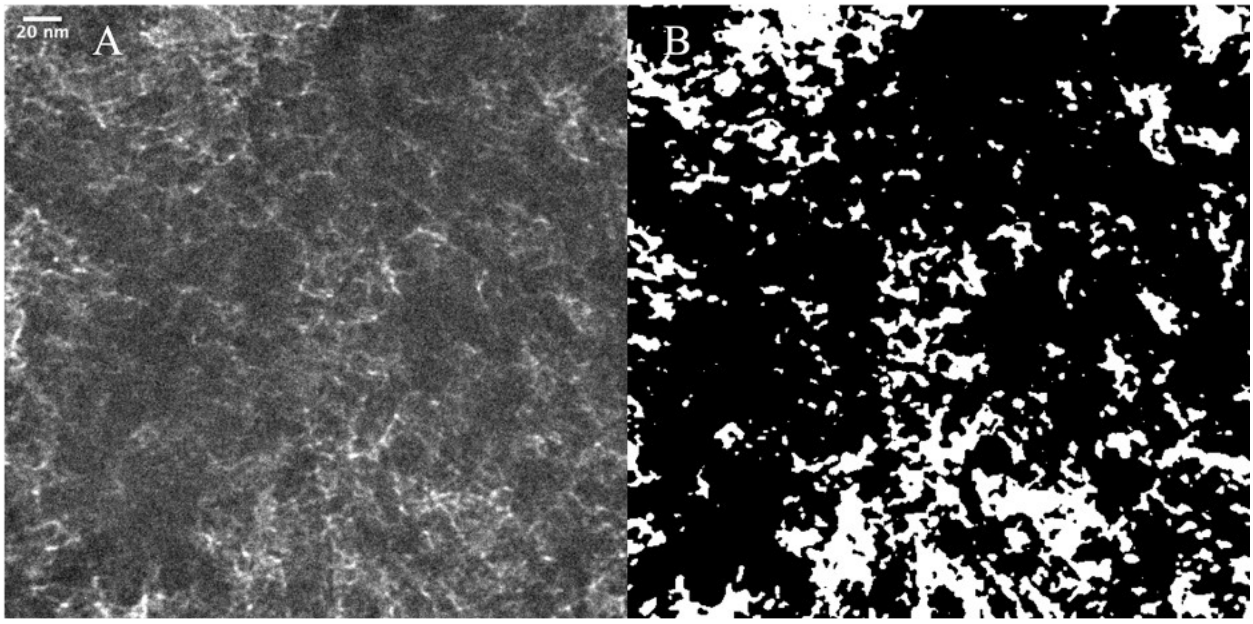

Figure S34: A TEM image (A) and the associated binary image (B) of the CZA at 11.5x magnification

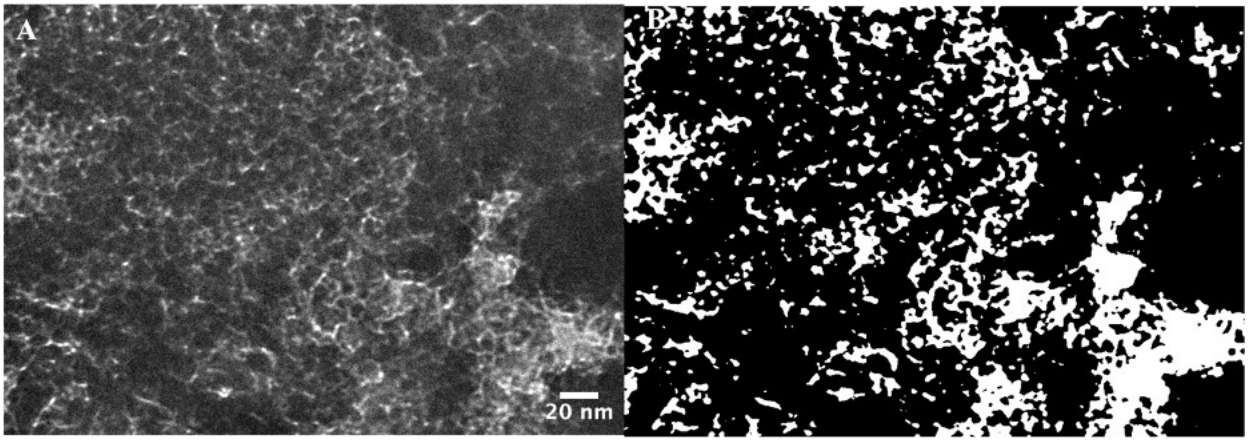

Figure S35: A TEM image (A) and the associated binary image (B) of the CZA at 19x magnification

Table S15: CZA pore size and porosity analysis of TEM images

Image	Count	Total Area (nm^2)	Average size (nm)	% Area
1288	286	5972.284	20.882	7.889
1326	786	8886.642	11.306	9.365
1312	944	15535.752	16.457	21.378
1311	246	3901.755	15.861	16.676
1308	545	18006.914	33.04	17.904
1301	350	11041.772	31.548	10.058
1328	961	13273.014	13.812	15.43
1312	537	17004.124	31.665	23.399
1298	138	2147.471	15.561	9.399
1324	504	9379.201	18.61	8.117
1299	327	5875.596	17.968	21.713
1317	629	11645.743	18.515	11.48
1291	364	8596.953	23.618	21.618
1305	221	2620.527	11.858	12.472
1323	389	11739.222	30.178	13.625
Average	**482**	**9708.465**	**20.725**	**14.702**